Catalytic Activities and Structural Properties of Horseradish Peroxidase Distal His42 → Glu or Gln Mutant†

Motomasa Tanaka,‡ Koichiro Ishimori,‡ Masahiro Mukai,§ Teizo Kitagawa,§ and Isao Morishima*,‡

Department of Molecular Engineering, Graduate School of Engineering, Kyoto University, Kyoto 606-01, Japan, and Institute for Molecular Science, Okazaki National Research Institutes, Myodaiji, Okazaki 444, Japan

Received April 21, 1997; Revised Manuscript Received June 12, 1997⊗

ABSTRACT: The distal histidine (His) is highly conserved in peroxidases and has been considered to play a major role as a general acid-base catalyst for peroxidase reaction cycle. Recently, however, the X-ray structure of chloroperoxidase from the marine fungus *Caldariomyces fumago* has revealed that a glutamic acid is located at the position where most of the peroxidase has a histidine residue, suggesting that the carboxyl group in the glutamic acid (Glu) can also assist cleavage of an O−O bond in peroxides [Sundaramoorthy, M., Terner, J., & Poulos, T. L. (1995) *Structure 3*, 1367−1377]. In order to investigate catalytic roles of the glutamic acid at the distal cavity, two horseradish peroxidase mutants were prepared, in which the distal His42 has been replaced by Glu (H42E) or Gln (H42Q). The formation rate of compound I in the H42E mutant was significantly greater than that for the H42Q mutant, indicating that the distal Glu can play a role as a general acid-base catalyst. However, the peroxidase activity of the H42E mutant was still lower, compared to that for native enzyme. On the basis of the CD, resonance Raman, and EPR spectra, it was suggested that the basicity of the distal Glu is lower than that of the distal His and the position of the distal Glu is not fixed at the optimal position as a catalytic amino acid residue, although no prominent structural changes around heme environment were detected. The less basicity and improper positioning of the distal Glu would destabilize the heme−H_2O_2−distal Glu ternary intermediate for the peroxidase reaction. Another characteristic feature in the mutants was the enhancement of the peroxygenase activity. Since the peroxygenase activity was remarkably enhanced in the H42E mutant, the distal Glu is also crucial to facilitate the peroxygenase activity as well as the enlarged distal cavity caused by the amino acid substitution. These observations indicate that the distal amino acid residue is essential for function of peroxidases and subtle conformational changes around the distal cavity would control the catalytic reactions in peroxidase.

Horseradish peroxidase (HRP)[1] is a member of the plant peroxidase superfamily and one of the archetypal heme-containing peroxidases, which utilizes hydrogen peroxide (H_2O_2) or alkyl peroxide to oxidize a wide variety of organic and inorganic compounds. The most abundant isoenzyme, HRP C, has a molecular mass of 42 kDa and consists of 308 residues (Welinder, 1979), which contains a single protoporphyrin IX as a prosthetic group, two calcium ions (Haschke & Friedhoff, 1978; Ogawa et al., 1979; Morishima et al., 1986), four disulfide bonds, and eight N-linked carbohydrate chains (Clarke & Shannon, 1976). It catalyzes one-electron oxidation of various small substrates to free radical products, most notably, the conversion of phenols to phenoxy radicals (Dunfold, 1991). The catalytic cycle of HRP has been well established as below.

$$\text{resting state} + H_2O_2 \rightarrow \text{compound I} + H_2O \quad (1)$$

$$\text{compound I} + AH_2 \rightarrow \text{compound II} + AH\cdot \quad (2)$$

$$\text{compound II} + AH_2 \rightarrow \text{resting state} + AH\cdot \quad (3)$$

The resting ferric enzyme first reacts with H_2O_2 to yield a green intermediate, compound I (1). Compound I has oxyferryl iron (Fe^{IV}═O) and porphyrin π-cation radical with an overall oxidation state of +5 for the heme prosthetic group, 2 oxidizing equiv higher than that of the resting state. In the next steps, 2 and 3, compound I is reduced by a substrate, AH_2, to the resting state in two sequential one-electron transfer events *via* a second active intermediate, compound II. Compound II also contains an oxyferryl center in which the π-cation radical of compound I has been reduced.

Figure 1 shows the heme environmental architecture of the active site in cytochrome *c* peroxidase (C*c*P) (Finzel et al., 1984). In amino acid residues in the heme cavity, histidine (His) 42, distal His, is one of the key catalytic amino acid residues. The distal His is highly conserved in the active centers of most of peroxidases (Finzel et al., 1984; Poulos et al., 1993; Edwards et al., 1993; Kunishima et al., 1994; Sundaramoorthy et al., 1994; Petersen et al., 1994; Fukuyama

† This work was supported by grants-in-aid for scientific research from the Ministry of Education, Science, Culture and Sports (08249102, 07309006 to I. M.).

* To whom correspondence should be addressed. Phone: +81-75-753-5921. Fax: +81-75-751-7611. E-mail: morisima@mds.moleng.kyoto-u.ac.jp

‡ Kyoto University.

§ Institute for Molecular Science.

⊗ Abstract published in *Advance ACS Abstracts,* August 1, 1997.

[1] Abbreviations: HRP, horseradish peroxidase isozyme C; C*c*P, cytochrome *c* peroxidase; CPO, chloroperoxidase from the marine fungus *Caldariomyces fumago*; PCR, polymerase chain reaction; SDS−PAGE, sodium dodecyl sulfate−polyacrylamido gel electrophoresis; native HRP, peroxidase isolated from horseradish, isoenzyme C; wild-type HRP, recombinant horseradish peroxidase isozyme C expressed in *Escherichia coli*.

S0006-2960(97)00906-9 CCC: $14.00

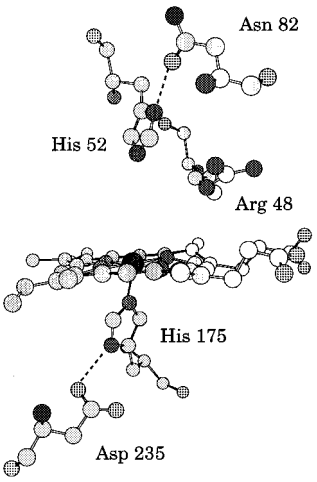

FIGURE 1: Heme environmental architecture of C*c*P. The residues equivalent to the catalytic Arg48, His52, Asn82, His175, and Asp235 are Arg38, His42, Asn70, His170, and Asp247 in HRP. Key hydrogen bonds in the crystal structure of the ferric enzyme are shown as dashed lines.

Scheme 1: Plausible Mechanism for Compound I Formation (Poulos & Kraut, 1980)

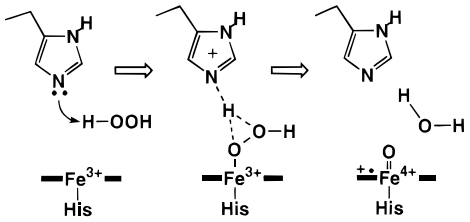

et al., 1995; Patterson & Poulos., 1995; Schuller et al., 1996) and has been considered to play a major role as a general acid-base catalyst in formation of compound I. Poulos and Kraut (1980) proposed that the distal His assists formation of the initial Fe−OOH complex by deprotonating an approaching H_2O_2 as a base and the following heterolytic cleavage of the O−O bond by protonating to the departing distal oxygen as an acid (Scheme 1).

Recent studies with mutant peroxidase have been conducted to investigate the roles of the distal His. The replacement of His52 by Leu in C*c*P has profound effects on the rate of compound I formation, the apparent bimolecular rate constant being decreased by 5 orders of magnitude relative to the value for native enzyme (Erman et al., 1992, 1993). In HRP, the mutants in which the distal His is replaced by Ala, Val, or Leu also exhibited extremely low reactivity to H_2O_2 (Newmyer & Ortiz de Montellano, 1995; Rodriguez-Lopez et al., 1996). We have demonstrated that small structural perturbation around the distal His can seriously decrease the peroxidase activity (Nagano et al., 1995, 1996; Tanaka et al., 1997). Thus, it has been concluded that peroxidase activity requires a His residue at the specific position as an effective acid-base catalyst.

Recently, however, X-ray structural analysis for one peroxidase, chloroperoxidase from the marine fungus *Caldariomyces fumago* (CPO), has shown that CPO bears a glutamic acid (Glu) at the distal cavity instead of the distal His. Although CPO has a different axial ligand from other peroxidases, the intermediate species during the catalytic reaction are assumed to be the same as those of other peroxidases (Dawson & Sono, 1987). In several enzymes such as β-glucosidase (MacLeod et al., 1994), a Glu residue has been also known to function as a general acid-base catalyst. However, functional roles of the Glu residue as a catalytic amino acid residue have never been examined in detail.

In order to elucidate functional and structural differences between distal His and Glu in peroxidases, we have prepared a HRP mutant in which the distal His at the position of 42 has been replaced by Glu (H42E) (Tanaka et al., 1996). Although the reaction rate with H_2O_2 (formation rate of compound I) for the H42E mutant was retarded by the mutation, the activity was distinctively higher than those of mutants having Ala or Val at the position for the distal His (Newmyer & Ortiz de Montellano, 1995), demonstrating that the distal Glu in H42E mutant can facilitate the reaction with H_2O_2 as a general acid-base catalyst.

In this paper, to get further insight into the catalytic role of the distal Glu in H42E mutant, we examined functional and structural alterations by the mutation at the distal His to Glu. In addition to the replacement of the distal His by Glu, we also substituted the His for Gln (H42Q) to access the role of the carboxylate group in the Glu residue. CD, EPR, and resonance Raman spectroscopies were utilized in this study to characterize the heme environmental structure of the mutants. We also investigate not only the peroxidase activity of the mutants through the elementary reaction rate constants in the reaction cycle but also the peroxygenase activity for thioanisole sulfoxidation and styrene epoxidation.

EXPERIMENTAL SECTION

Materials. Native HRP, type VI, was purchased from Sigma as a lyophilized and salt-free powder and used without further purification; the protein is predominantly isozyme C. The native enzyme exhibited an A_{402}/A_{280} ratio (RZ value) of 3.2. General molecular biology supplies were obtained from Takara and Perkin-Elmer. All buffer materials and other chemicals were purchased from Wako and Nakarai Tesque as the highest quality available.

Site-Directed Mutagenesis. Site-directed mutagenesis of recombinant HRP C at the position of 42 was carried out by the use of the polymerase chain reaction (PCR)-based technique with T7 HRP as a template (Nagano et al., 1995, 1996). To construct the insert DNA fragment with mutation (His 42 → Glu or Gln), the synthetic oligonucleotide 5′-GAAGCAGTCCTCGAAGTGCAG-3′ (H42E) or 5′-GAAGCAGTCTTGGAAGTGCAG-3′ (H42Q) was used as a primer to multify mutated DNA fragments. The amplified DNA fragments bearing the mutation were then ligated into the wild-type gene by utilizing the unique *Nde*I and *Bgl*II restriction enzyme sites in T7 HRP vector. The ligation mixture was used to transform *Escherichia coli* strain BL 21 with ampicillin resistance. Positive clones were screened by SDS−PAGE, and introduction of the mutation was verified by double-stranded DNA sequence analysis using the dideoxy chain termination method with 373 DNA sequencer (Applied Biosystems). No additional mutations in the mutated HRP gene were detected.

Expression, Reconstitution, and Purification of HRP. The wild-type and mutant HRPs were expressed in *E. coli* strain BL 21 and extracted from inclusion bodies as described previously by Nagano et al. (1996). Reactivation of apoHRP in the presence of calcium and heme and purification of holoHRP was followed by the method of Smith et al. (1990) and Gazaryan et al. (1995) with some modifications.

The RZ values of wild-type and mutant HRPs obtained finally were about 3.2 and 4.0, respectively. Peroxidase concentration was estimated by using of the Soret extinction coefficient in the pyridine hemochrome form (Paul et al., 1953). The extinction coefficients were 102, 103, 115, and 109 mM^{-1} cm^{-1} for native, wild-type, H42E, and H42Q mutant HRPs, respectively.

Elementary Reaction Rates in the Catalytic Cycle. Formation and reduction of compound I were monitored on a stopped-flow spectrophotometer (UNISOKU) at 25.0 °C in 50 mM sodium phosphate buffer, pH 7.0. HRP (2.0 μM) was used to determine the elementary reaction rate constants. More than 10-fold excess of H_2O_2 or substrates (guaiacol and ferrocyanide) relative to the HRP concentration was used to ensure pseudo-first-order kinetics. Formation (k_1) and reduction (k_2) rates of compound I were measured by following decrease of the absorbance at 395 nm and increase of the absorbance at 412 nm, respectively. A solution of native compound I was prepared just before the kinetics measurements by adding a slight excess of H_2O_2 to the ferric enzyme solution. In case of H42E, the k_2 measurement was carried out in 10 min after adding a slight excess of H_2O_2 to yield enough amount of compound I. Rate constants were determined by fitting the recorded data by using an IgorPro program (WaveMetrics). Due to instability of mutant compounds II at neutral pH (Tanaka et al., 1996), the reduction rates of compounds II, k_3, could not be measured by the stopped-flow technique. The k_3 value was calculated by using k_1 and k_2 values and an overall reaction rate under the steady-state condition (V). The overall reaction rate is represented as below (Cormier & Prichard, 1968; Hasinoff & Dunfold, 1970).

$$V = (2k_1k_2k_3[\text{HRP}][\text{substrate}][H_2O_2])/\{(k_1k_2 + k_1k_3)[H_2O_2] + k_2k_3[\text{substrate}])\} \quad (4)$$

Peroxygenase Activity: Sulfoxidation of Thioanisole. The reaction of the enzyme (1−10 μM) and thioanisole (1 mM) in 50 mM sodium phosphate buffer (pH 7.0) at 25.0 °C was initiated by the addition of H_2O_2 (1 mM). Incubation at 25.0 °C was stopped at various time points, then the product was purified, followed by the analysis as described below. At first, the solution was extracted with CH_2Cl_2 and acetophenone was added as a standard to a final concentration of 0.1 mM. The extracts were concentrated nearly to dryness under a stream of argon. The residue taken up in the HPLC solvent was analyzed by isocratic HPLC on a Daicel chiral column installed on a Shimadzu SPD-10A spectrophotometer equipped with a Shimadzu LC-10AD solvent pump system. The column was eluted with 85% hexane and 15% isopropyl alcohol at a flow rate of 0.5 mL/min. The HPLC effluent was monitored at 254 nm. The retention time for the *S* and *R* isomers of methyl phenyl sulfide were 21.1 and 24.7 min, respectively. The methylphenyl sulfide enantiomers were identified by chromatographic comparison with authentic (*R*)-methyl phenyl sulfide and racemic methyl phenyl sulfide. The linearity of the relationship between time and product formation was confirmed in the assay. In the control experiments, thioanisole was oxidized nonenzymatically at a rate of 0.6 pmol s^{-1} at 25.0 °C. This background level has been subtracted from the experimentally determined values in calculating the enzymatic rates and enantiomeric excesses.

Peroxygenase Activity: Epoxidation of Styrene. Five microliters of the 10 mM H_2O_2 solution was added to a 0.5 mL of sodium phosphate buffer (pH 7.0) solution containing 20 mM HRP and 10 mM styrene to initiate the epoxidation reaction. The experimental procedure was the same as that for sulfoxidation of thioanisole. The residue was analyzed by gas−liquid chromatography on a Shimadzu GAS CHROMATOGRAPH GC-14A equipped with a 0.25 mm × 30 m Chiraldex G-TA capillary column (Advanced Separation Technologies, Whippany, NJ). The column temperature was kept at 100 °C during the analysis. 2-Phenyl-2-propanol was used as a standard. The retention times of (*S*)- and (*R*)-styrene oxide were 9.7 and 12.7 min, respectively. The styrene oxide enantiomers were identified by chromatographic comparison with authentic (*R*)-styrene oxide and racemic styrene oxide. Nonenzymatic styrene epoxidation was observed under these conditions.

Circular Dichroism (CD) Spectroscopy. CD spectra of HRPs were measured with JASCO J-720 at room temperature. Mean residue α-helical contents were evaluated from the mean residue ellipticity at 222 nm by following the equation (Greenfield & Fasman, 1969)

$$\alpha\text{-helix}\ (\%) = -([\theta]_{222} + 2340)/30300 \quad (5)$$

In the course of the measurement, nitrogen gas was purged into the cell room in order to avoid incorporation of chirality by dioxygen in the air. CD spectra reported in this paper were an average of eight scans recorded at a speed of 100 nm/min and a resolution of 0.2 nm. Concentration of HRP was *ca.* 5 μM, and the light path of a sample cell was 1 mm.

Electron Paramagnetic Resonance (EPR) Spectroscopy. EPR spectra of HRPs were measured on a Varian E-12 spectrometer equipped with an Oxford ESR-900 liquid helium cryostat. Measurements were carried out at the X-band (9.22 GHz) microwave frequency at 5 K. The sample concentration was *ca.* 200 μM HRPs and the volume was 100 mL. Compounds I of native and wild-type HRPs were prepared by adding a small excess of H_2O_2 to the ferric resting states. Mutant compounds I were generated by adding 5 or 100 equiv of H_2O_2 to the ferric H42E or H42Q mutant solution, respectively. The sample was frozen in quartz EPR tubes by submersion in liquid nitrogen over a period of 1 min immediately after addition of H_2O_2 to native or wild-type HRP. For the mutants, the reaction mixture was incubated for 10 min at room temperature to yield enough amount of mutant compounds I. EPR spectra were recorded at 5 K.

Resonance Raman Spectroscopy. Resonance Raman spectra of HRPs were recorded with excitation from Kr^+ ion laser (Spectra Physics, Model 2016), using the 406.7 and 413.1 lines, and from He/Cd laser (Kinmon Electrics, Model CD 1805B), using the 441.6 nm line. The resonance Raman scattering was detected with a photodiode array (PAR 1421HQ) attached to a charge-coupled device (CCD) (PAR 1530-CUV) attached to a single monochrometer (Chromex 2510S). The slit width used here was 150 μm. Resonance Raman spectra were acquired with a spinning quartz cell at room temperature, except for compound II. The measurements for compound II were acquired at about 10 °C by flowing cooled nitrogen gas to the sample cell. The frequency calibration was performed with indene (500−1650

Table 1: Elementary Reaction Rate Constants (M^{-1} s^{-1}) of Native, Wild-Type, H42E and H42Q HRPs at pH 7.0 and 25.0 °C

HRP	k_1	k_2 (guaiacol)	k_2 (ferrocyanide)	k_3[a]
native	1.4×10^7	6.9×10^6	2.8×10^6	1.3×10^6
wild-type	1.4×10^7	5.9×10^6	5.4×10^6	1.2×10^6
H42E	4.9×10^3	7.7×10^5	7.2×10^6	7.9×10^3
H42Q	9.6×10^1	ND[b]	ND	ND

[a] k_3 was determined with guaiacol as a reductant. [b] ND denotes not determined.

Table 2: Peroxygenase Activities ($nmol^{-1}$ s^{-1} μmol^{-1}) of Native, Wild-Type, H42E and H42Q HRPs at pH 7.0 and 25.0 °C

HRP	thioanisole (%S)	styrene (%S)
native	8.0 (52)	trace
wild-type	48 (61)	0.057 (15)
H42E	2.6×10^3 (45)	40 (15)
H42Q	16 (36)	0.69 (53)

cm^{-1}) or carbon tetrachloride (200−500 cm^{-1}) as a standard. Native and wild-type compounds II were prepared by adding a slight excess of H_2O_2 to the ferric solutions. H42E and H42Q compounds II were prepared by addition of 5 and 100 equiv of H_2O_2, respectively. Sodium phosphate buffer at pD 7.0 and borate buffer at pD 10.0 were used in the measurements. $H_2{}^{18}O_2$ was prepared from $^{18}O_2$ as described by Sawaki and Foote (1979). Ferrous HRPs were prepared by addition of a small volume of a freshly saturated sodium dithionite solution to degassed ferric solutions. The pH value in the HRP solution was exactly corrected after the addition of the sodium dithionite solution. A cyanide-ligated form of HRP was prepared by mixing 100 equiv of potassium cyanide solution with a ferric HRP solution in 50 mM sodium phosphate buffer at pH 7.0. The pH value in the HRP solution was not changed after the addition of the potassium cyanide solution.

Redox Potential of Fe^{2+}/Fe^{3+} Couple. The redox potentials of HRPs were monitored with platinum electrode and a Shimadzu MPS-2000 UV−vis spectrophotometer. The mediator used here was a mixture of safranine T, phenosafranine, benzylviologen, and α-hydroxyphenazine. The ferric HRPs were photoreduced in a 50 mM potassium phosphate buffer (pH 7.0) containing 50 mM EDTA (Makino et al., 1982). The midpoint potential of HRP (E_0) was determined from a plot of E_h against the logarithm of percentage reduction of HRP using eq 6 below (Yamada et al., 1975).

$$E_h = E_0 + (RT/\nu F)\ln\{[\text{oxidized HRP}]/[\text{reduced HRP}]\} \quad (6)$$

In the equation, ν and F denote number of electron involved in the redox reaction and Faraday constant, respectively. The midpoint potential of HRP was corrected by utilizing phenosafranine (−252 mV) as a standard.

RESULTS

Peroxidase Activity. The second-order rate constants for the reaction with H_2O_2 or substrate were summarized in Table 1. The formation rates of compound I (k_1) for native and wild-type HRPs (1.4×10^7 M^{-1} s^{-1}) are in close agreement with values reported by Smith et al. (1992). The replacement of the distal His with Glu or Gln gave a substantial effect on the k_1 value, depressing it to 4.9×10^3 or 9.4×10^1 M^{-1} s^{-1}, respectively. The k_1 value for the H42E mutant was, however, still significantly larger than that of another mutant, H42Q. The H42Q mutant exhibited a very small k_1 value as observed for H42L mutant in which the distal His was substituted for Leu (Rodriguez-Lopez et al., 1996).

The reduction rate of compound I (k_2) was examined by using two types of substrates. One is guaiacol, which is a proton and an electron donor to HRP, and another is ferrocyanide, which is only an electron donor to HRP. The k_2 value for native HRP (6.9×10^6 M^{-1} s^{-1}) to guaiacol is approximately in accord with the values reported by Yamazaki et al. (1973) (9×10^6 M^{-1} s^{-1}). In contrast to the k_1 value, the k_2 value for the reaction of H42E mutant with guaiacol (7.6×10^5 M^{-1} s^{-1}) were not so much different from those of native and wild-type HRPs. Deviations in the k_2 value for the H42E mutant to ferrocyanide (8.7×10^5 M^{-1} s^{-1}) from those for native (2.8×10^6 M^{-1} s^{-1}) and wild-type HRPs (5.4×10^6 M^{-1} s^{-1}) were also small. k_2 values for the H42Q mutant could not be obtained due to the extremely low k_1 value.

Since compound II for the H42E mutant at neutral pH was quite unstable (Tanaka et al., 1996), the reduction rate of compound II (k_3) could not be measured by the stopped-flow technique. The k_3 value was estimated by eq 4 (Cormier & Prichard, 1968; Hasinoff & Dunfold, 1970). The k_3 value of the H42E mutant for guaiacol was decelerated to 7.9×10^3 M^{-1} s^{-1} as listed in Table 1.

Peroxygenation Activity. The sulfoxidation activity of thioanisole was assayed, and the activities of HRPs are listed in Table 2. The higher activity of wild-type HRP compared with that of native protein suggests that the glycosylation in native HRP is an obstacle to the incorporation of a substrate, which was supported by the low sulfoxidation activity of polyhistidine-tagged HRP (Newmyer & Ortiz de Montellano, 1995). While the activity of the H42Q mutant was as low as that of wild-type HRP, the H42E mutant aquired extremely high activity (2.6×10^3 $nmol^{-1}$ s^{-1} μmol^{-1}), and the activity was superior to that of P450cam (58 $nmol^{-1}$ s^{-1} μmol^{-1}) (Fruetel et al., 1994; Newmyer & Ortiz de Montellano, 1995). The preferred *S* enantioselectivities of the distal His mutants were relatively low (H42E, 45%; H42Q, 36%) compared with that of wild-type HRP (61%).

We also examined the epoxidation activity of styrene as summarized in Table 2. The activity of wild-type HRP was significantly higher than that of native enzyme, indicating that the glycosylation affected the epoxidation reaction. The H42Q mutant exhibited a little higher activity than wild-type HRP, whereas H42E mutant was a much better epoxidation catalyst than wild-type enzyme. The activity of the H42E mutant (40 $nmol^{-1}$ s^{-1} μmol^{-1}) is still higher than that of P450cam (18 $nmol^{-1}$ s^{-1} μmol^{-1}) (Fruetel et al., 1992; Newmyer & Ortiz de Montellano, 1995). The preferred *S* enantioselectivity of styrene oxidation of the H42E mutant (15%) is similar to that of wild-type HRP (15%), while that of the H42Q mutant showed the quite higher enantioselectivity (53%).

CD Spectroscopy. Figure 2 depicts CD spectra of ferric native, wild-type, H42E and H42Q HRPs, and Table 3 collects their α-helical contents (%) from eq 5. The spectral shapes of the mutant HRPs are almost identical to those of native and wild-type HRPs, and the α-helical content is also insensitive to the amino acid substitution at the distal His as

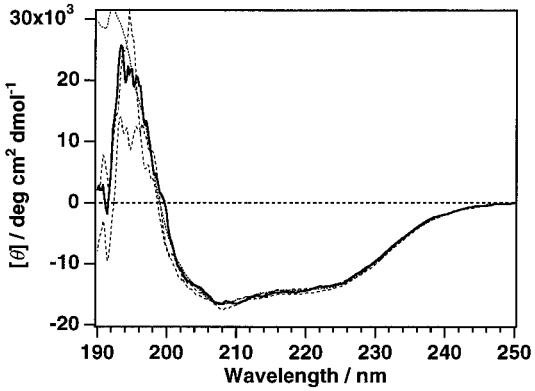

FIGURE 2: Circular dichroism spectra of resting state native (thick line), wild-type (thin line), H42E (broken line), and H42Q (dotted line) HRPs in 50 mM sodium phosphate buffer at pH 7.0.

Table 3: Mean Residue Molar Ellipticities at 222 nm and Estimated α-Helical Contents of native, wild-type, H42E and H42Q HRPs in their Resting States

HRP	$-[\theta]_{222} \times 10^{-4}$ [a]	α-helix (%)
native	1.37	37
wild-type	1.45	40
H42E	1.39	38
H42Q	1.41	39

[a] Mean residue ellipticity in deg cm^2 dmol^{-1}.

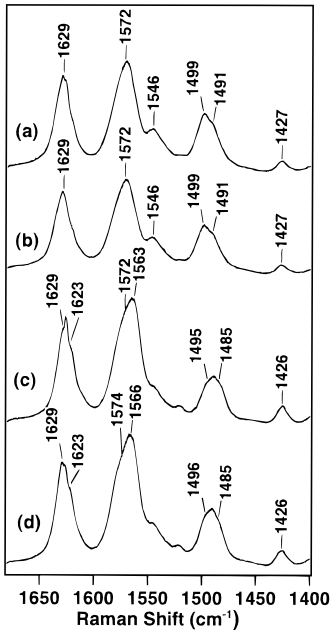

FIGURE 3: Resonance Raman spectra of resting state of (a) native, (b) wild-type, (c) H42E, and (d) H42Q HRPs at pH 7.0 by 406.7 nm excitation. Laser power, 10 mW; accumulation time, 4 min; enzyme concentration, 30 μM.

listed in Table 3. These results indicate that the mutants are refolded properly as is native enzyme.

Resonance Raman Spectroscopy. The high-frequency region of the resonance Raman spectra of the resting state HRPs by 406.7 nm excitation is shown in Figure 3. As previously reported for native HRP (Smulevich et al., 1994), the characteristic bands at 1499, 1572, and 1629 cm^{-1} has been assigned to the 5-coordinate high-spin state (5-cHS). In the spectra of the H42E and H42Q mutants, extra Raman bands at 1485, 1563, and 1623 cm^{-1} appeared in the ν_3, ν_2, and $\nu_{C=C}$ regions, respectively. These spectral features were also encountered in F41V and F41W mutants (Smulevich et al., 1994), which contain the 6-coordinate high-spin (6-cHS) species in their resting states.

Figure 4 provides resonance Raman spectra of native, wild-type, and mutant compounds II with 406.7 nm excitation. The Raman band at 775 cm^{-1} in the spectrum of native HRP has been attributed to the Fe^{IV}═O stretching vibration mode in compound II. The corresponding stretching mode was observed at 789 cm^{-1} for the mutants (Figure 4A). Although the isotope shift for ^{18}O was not clear in Figure 4B, the difference spectra (Figure 4C) clearly show that the mutation induces an upshift of the $\nu_{Fe=O}$ Raman band from 776 cm^{-1} (native and wild-type HRPs) to 788 cm^{-1}. The Raman shifts of the mutants at pD 7.0 were comparable with that of native HRP at pD 10.0 (785 cm^{-1}) (data not shown). The intensity of the $\nu_{Fe=O}$ Raman line in mutant compounds II is small, corresponding to the destabilized compounds II at neutral pH as previously reported (Tanaka et al., 1996).

Figure 5 illustrates resonance Raman spectra of (A) $C^{14}N$, (B) $C^{15}N$-ligated states, and (C) their difference spectra with 413.1 nm excitation. The Raman band at 451 cm^{-1} of native cyanide-ligated HRP has been assigned to the axial Fe−CN stretching Raman frequency (Al-Mustafa & Kincaid, 1994). Although the corresponding Raman bands for the cyanide-ligated H42E and H42Q mutants were almost diminished, as shown in Figure 5A, the difference spectra (Figure 5C) clearly showed an isotope shift of the Fe−CN mode. The Raman shifts in the H42E (443 cm^{-1}) and H42Q (443 cm^{-1}) mutants were lower by about 13 cm^{-1} than those in native (456 cm^{-1}) and wild-type (456 cm^{-1}) HRPs, indicating the significant perturbation of the Fe−CN bond in cyanide-ligated forms of the mutants. Such a lower frequency was also found for native HRP at high pH (444 cm^{-1} at pH 12.5), where the distal His does not make a hydrogen bond with the heme-bound cyanide due to deprotonation of the distal His (Al-Mustafa & Kincaid, 1994).

Figure 6 displays the low-frequency region in resonance Raman spectra of ferrous HRPs with 441.1 nm excitation. The spectra of reduced native and wild-type HRPs are characterized by a strong band at 242 cm^{-1}, which has been assigned to the stretching mode between the ferrous iron and the N_ϵ atom of the anionic proximal imidazole (His 170) (Teraoka & Kitagawa, 1981). In the spectra of the H42E and H42Q mutants, the Raman band of Fe^{II}−His exhibited downshift by 3 cm^{-1}, indicating that the Fe^{II}−His bond in the ferrous states of the mutants is weakened by the amino acid substitution at the distal His, while all other bands did not exhibit a detectable frequency shift.

The pH-dependent profile of Fe^{II}−His bond is shown in Figure 7, and the pK_a values are summarized in Table 4. The pK_a values for native (7.4) and wild-type HRPs (7.0) correspond to the value (7.17) reported by Teraoka and Kitagawa (1981). Although the pK_a value for the H42E mutant might not be so accurate due to small pH dependence of the Fe^{II}−His Raman frequency, the pK_a value (4.6) was apparently decreased from that of wild-type HRP (7.0). Since the pK_a value has been considered to be correlated with the basicity of the distal His (Teraoka & Kitagawa, 1981; Mukai et al., 1997), the basicity of the distal Glu in the H42E mutant was substantially depressed relative to those of the distal His in native and wild-type enzymes. We could not determine the pK_a value for the H42Q mutant due to the unclear sigmoidal curve in the pH titration.

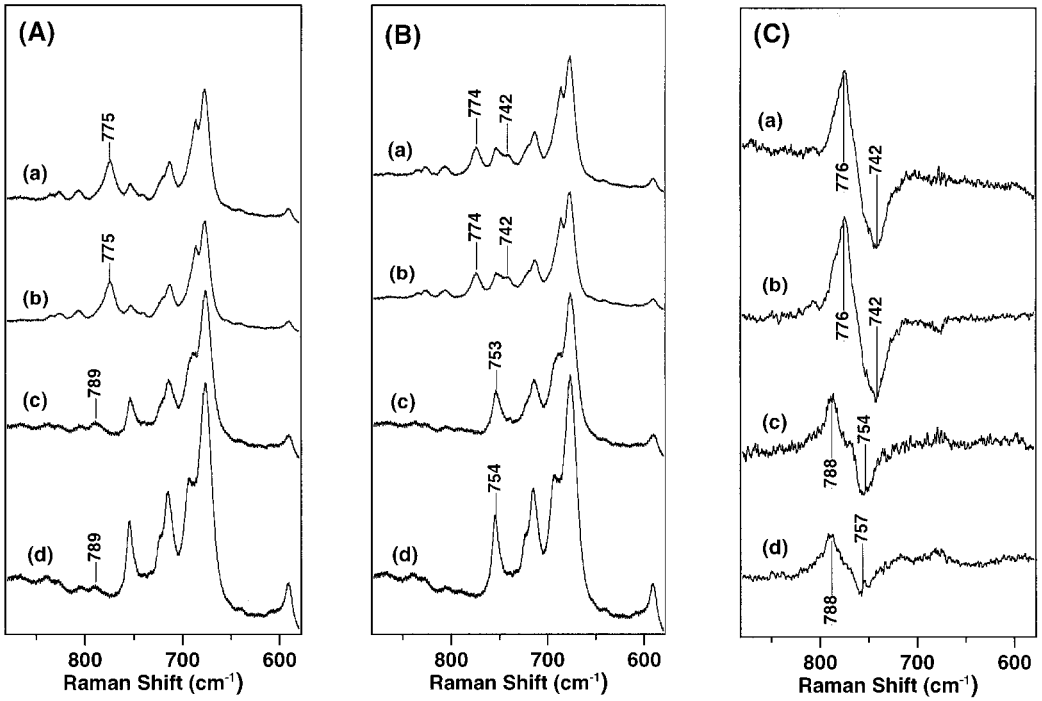

FIGURE 4: Resonance Raman spectra of compounds II of (a) native, (b) wild-type, (c) H42E, and (d) H42Q HRPs in D_2O buffer at pD 7.0 by 406.7 nm excitation. Laser power, 4 mW; accumulation time, 2 min; enzyme concentration, 30 μM. (A) compound II derived from $H_2{}^{16}O_2$ (B) compound II derived from $H_2{}^{18}O_2$ (C) $H_2{}^{16}O_2-H_2{}^{18}O_2$

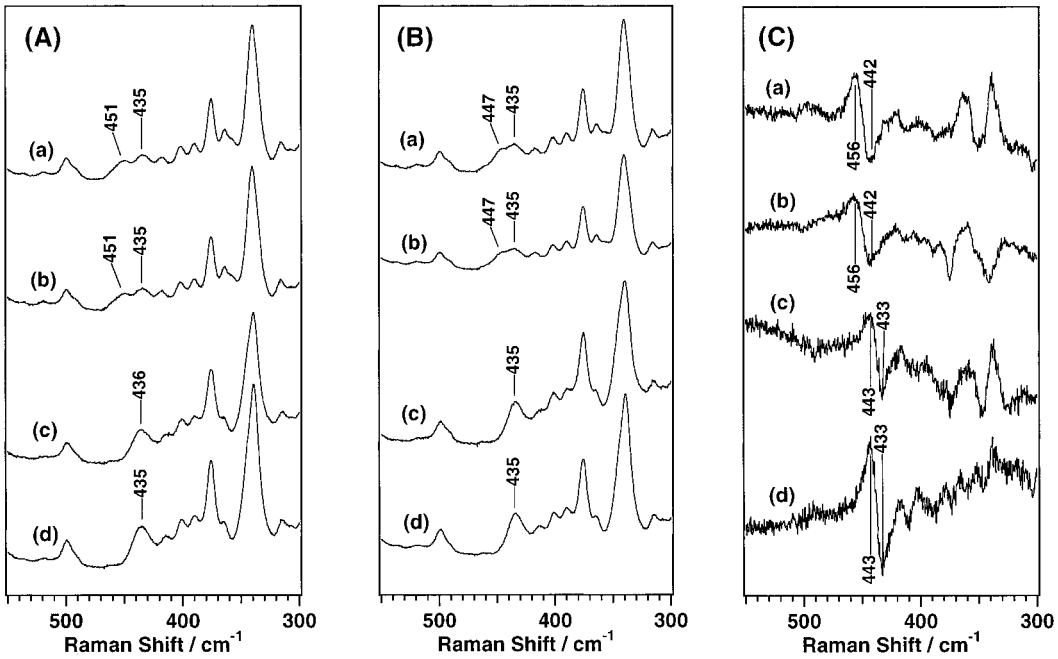

FIGURE 5: Resonance Raman spectra of cyanide-ligated state of (a) native, (b) wild-type, (c) H42E, and (d) H42Q HRPs at pH 7.0 by 413.1 nm excitation. Laser power, 20 mW; accumulation time, 3 min; enzyme concentration, 50 μM. (A) $C^{14}N$, (B) $C^{15}N$, and (C) $C^{14}N-C^{15}N$.

EPR Spectroscopy. Figure 8A presents EPR spectra of resting states of HRPs. Native and wild-type HRPs exhibited almost identical spectral basis with prominent rhombic high-spin splitting. The splitting for the H42E and H42Q mutants was smaller than those of native and wild-type HRPs, implying some improvement of the symmetry around the heme in the mutants, probably due to contribution of 6-cHS species. EPR spectra of compounds I were illustrated in Figure 8B. A broadened featureless peak at $g = 2$ in the spectra of native and wild-type compounds I have been attributed to the porphyrin π-cation radical (Schulz et al., 1979), and a peak at $g = 6$ is derived from a small component of ferric high-spin species. The broad signal at $g = 2$ was clearly detected in both of the mutant compounds I, indicating that the mutants can yield compound I. An additional peak at $g = 4.3$, arising from the degraded heme, appeared in the EPR spectrum of the H42Q mutant.

Redox Potential of Fe^{2+}/Fe^{3+} Couple. The redox potentials of Fe^{2+}/Fe^{3+} couple are compiled in Table 5. The value of -260 mV of native enzyme coincided with the value (-278 mV) reported by Makino et al. (1975). The redox potentials of the mutant HRPs (H42E, -278 mV; H42Q, -260 mV) were almost the same as those of native and wild-type HRPs, suggesting that the electronic donation from

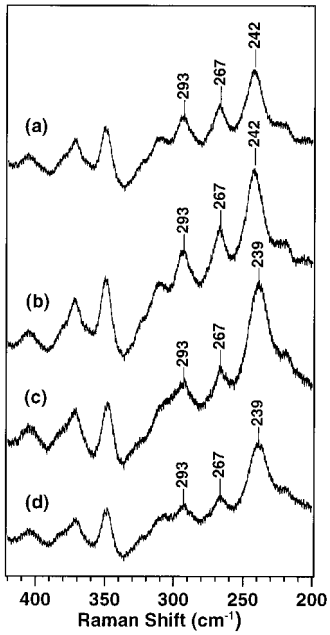

FIGURE 6: Resonance Raman spectra of ferrous state of native, wild-type, H42E, and H42Q HRPs at pH 7.0 by 441.6 nm excitation. Laser power, 14 mW; accumulation time, 4 min; enzyme concentration, 50 μM.

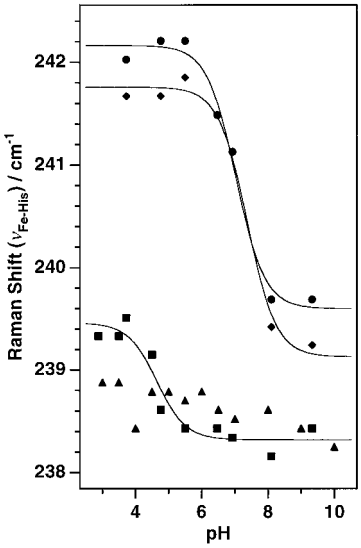

FIGURE 7: The pH dependences of the Fe^{II}−His stretching frequencies of ferrous native (●), wild-type (◆), H42E (■), and H42Q (▲) HRPs. The solid line represents theoretical curves expected for dissociation of one proton.

Table 4: pK_a Value of Distal Residues in HRPs Proved by pH-Dependent Resonance Raman Shift of Fe^{II}−His Bond

HRP	pK_a
native	7.4
wild-type	7.0
H42E	4.6
H42Q	ND[a]

[a] ND denotes not determined.

proximal His to the heme iron in the mutants is quite similar to that of native HRP in the resting state.

DISCUSSION

Peroxidase Activity. As listed in Table 1, one of the most characteristic features in the peroxidase reaction of the H42E

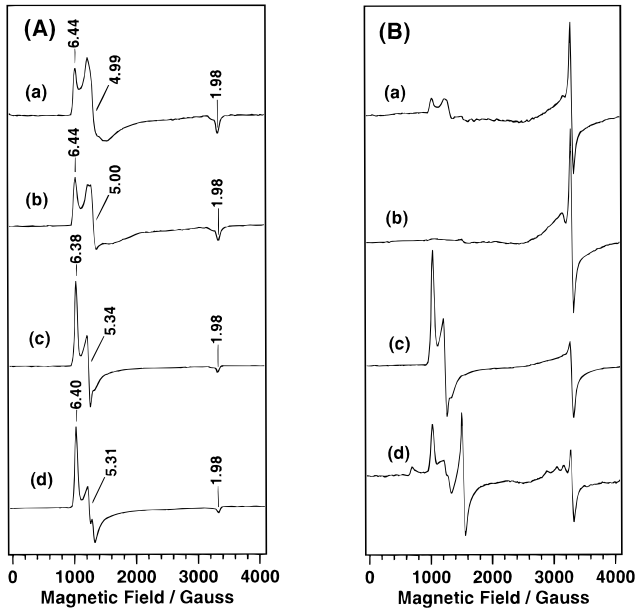

FIGURE 8: EPR spectra of (A) resting state and (B) compound I of (a) native, (b) wild-type, (c) H42E, and (d) H42Q HRPs in 50 mM sodium phosphate buffer at pH 7.0.

Table 5: Redox Potential (Fe^{2+}/Fe^{3+} Couple) of Native, Wild-Type, H42E and H42Q HRPs

HRP	E_h /mV
native	−266
wild-type	−258
H42E	−258
H42Q	−277

Scheme 2: Plausible Mechanism for Compound I Reduction (Dunfold, 1991)

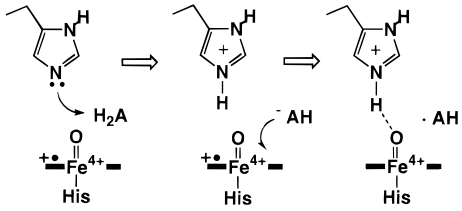

mutant is the preferential depression of k_1 and k_3. k_2 is almost insensitive to the amino acid replacement of the distal His by Glu. The k_2 process, which corresponds to the reduction of the compound I, has been considered to proceed as Scheme 2 (Dunfold, 1991) and consists of the two steps proton abstraction of the substrate and electron transfer. In native HRP, the electron transfer step is the rate-determining step (Job & Dunfold, 1976). Since the k_2 for the H42E mutant was not affected by the amino acid substitution at the distal position, the electron transfer process is independent of the mutation and still the rate-determining step. This finding is not so surprising, since the distal amino acid residue would not directly contribute to the electron transfer step as manifested in Scheme 2. It should be noted that the rate-determining step for the reaction by the H42E mutant is also the electron transfer step, which suggests that the proton abstraction by the distal Glu does not retard seriously.

On the other hand, the k_1 value of H42E mutant decreased greatly compared with those of native and wild-type enzymes. In the k_1 process (Scheme 1), formation of the heme−H_2O_2−distal His ternary complex has been considered to be a key step to yield compound I as well as the proton

abstraction by the distal amino acid residue (Dawson & Sono, 1987; Dunfold, 1991; Newmyer & Ortiz de Montellano, 1996). Since k_2 for the H42E mutant indicates that the proton-abstraction step is not dramatically perturbed by the mutation, it is plausible that the ternary complex as the reaction intermediate is unstable, resulting in the large deceleration in the k_1 process. The destabilization of the ternary complex in the H42E mutant is suggested by the resonance Raman spectra. As Figure 7 and Table 4 indicate, the pK_a for the H42E mutant is lower than that of the parent enzyme, which corresponds to the lower basicity of the distal Glu (Mukai et al., 1997) and would destabilize the ternary complex. The higher frequency shift of heme-bound cyanide (Figure 5) for the H42E mutant also implies that the hydrogen bond between the bound cyanide and the distal amino acid residue, which would stabilize the ternary complex, was disrupted in the mutant.

The heme environmental structure around the proximal His would be also one of determinants to the rapid reaction of peroxidase with H_2O_2 (Vitello et al., 1992). The strong electron donation from anionic proximal His to heme−iron facilitates the cleavage of the O−O bond in the k_1 process (Dunfold, 1991). The stretching mode between Fe^{II} and the proximal His (Figure 6) suggested that the electron donation in the H42E mutant is smaller than those in native and wild-type enzymes. However, such a little downshift of the iron−His stretching mode is encountered for our previous mutants (Mukai et al., 1997), in which k_1 values were not depressed so much as the H42E mutant. In the ^{1}H NMR spectrum of the ferric H42E mutant, the chemical shift of $N_\delta H$ from proximal His was identical to that from wild-type HRP, indicating that the electronic structure around the proximal His is not changed (Tanaka et al., 1996). These observation shows that the electron donation from proximal His is not responsible for the decrease in the reaction rate with H_2O_2 in the H42E mutant.

Although the heme environmental structure of the H42E mutant is almost the same as that of native enzyme, it is evident that the distal Glu cannot be fixed at the optimal position for the stable ternary complex formation by the interaction from the other amino acids. As we reported previously (Nagano et al., 1995, 1996; Tanaka et al., 1997), the mutation which perturbs interactions fixing the distal His at the optimal position for the peroxidase reaction drastically depressed the reaction rate of the k_1 process, even though the mutant has the distal His. In addition, our preliminary X-ray crystal analysis of the H42E mutant also suggested that the distal Glu moved away from the heme relative to the distal His in native enzyme. In particular, it would be noteworthy that the position of the O_ϵ atom from the distal Glu, which would be essential to form the formation of the ternary complex in the reaction, is quite different from that of the N_ϵ atom from the distal His in the parent enzyme. In the H42E mutant, therefore, we can conclude that the deceleration in the k_1 process is originated from not only the less basicity but also the improper position of the distal Glu for the formation of the stable ternary reaction intermediate.

It is also of interest that the k_1 value for CPO, in which a Glu residue is located at the distal cavity, is 2.3×10^6 M^{-1} s^{-1} (Sun et al., 1994), which is much higher than that of the H42E mutant (4.9×10^3 M^{-1} s^{-1}) and comparable to that of native HRP (1.4×10^7 M^{-1} s^{-1}). The crystal structure of CPO showed that the distal Glu is fixed in the position by a hydrogen bond with an adjacent His (Sundaramoorthy et al., 1995), as expected for native HRP (Nagano et al., 1995, 1996). In our previous studies (Nagano et al., 1995, 1996), the breakage of the hydrogen bond between the distal His and Asn70 in HRP induced severe functional defects in peroxidase activity. Therefore, the hydrogen bond which fixes the distal catalytic amino acid residue in peroxidase is crucial to locate the distal amino acid residue at the optimal position to play a role of a general acid-base catalyst. If the distal Glu in the mutant HRP is fixed at the optimal position by such a hydrogen bond like in CPO, the distal Glu would work as a more efficient general acid-base catalyst and the reaction rate with H_2O_2 could be improved.

The k_3 value, the reduction rate of compound II, of the H42E mutant was also discouraged by the mutation. One of the factors to determine the reaction rate for the reduction of compound II is reduction potential for compound II. Accelerated electron transfer from a substrate to compound II was observed for the peroxidase reaction mediated by *Arthromyces ramosus* peroxidase (Farhangrazi et al., 1994), which has high reduction potential for compound II. The HRP mutants (N70V and N70D) we prepared in the previous study (Nagano et al., 1996) also exhibited high reduction potential for compound II and thereby promoted the electron transfer step. Although the exact reduction potential of the H42E compound II could not be determined due to instability at neutral pH, the time-dependent profile of UV−vis spectra in the reaction of ferric H42E with H_2O_2 suggested that the reduction potential of H42E compound II is also much higher than wild-type compound II (Tanaka et al., 1996). The reduction potential for H42E compound II, therefore, cannot be responsible for the decrease of the k_3 value in the mutant.

The other key factor for the k_3 process is the hydrogen bond between a ferryl oxygen in compound II and the $N_\epsilon H$ atom of distal His, which has been believed to enhance the reactivity of compound II with a substrate (Sitter et al., 1985; Makino et al., 1986). As shown in Figure 4, the Fe^{IV}═O stretching Raman frequency for the H42E mutant was observed at 789 cm^{-1}, which is 14 cm^{-1} higher than that for native HRP. This shift corresponds to cleavage of the hydrogen bond between the ferryl oxygen and the distal Glu, since the Raman shift of the H42E compound II at neutral pH was comparable to that of native compound II at alkaline pH, in which the hydrogen bond was disrupted due to deprotonation of the distal His. In diacetylheme-substituted HRP, the Fe^{IV}═O stretching Raman frequency for its compound II is 9 cm^{-1} higher than that of native enzyme compound II and exhibits lower reactivity (Makino et al., 1986).

The absence of the hydrogen bond between the distal amino acid residue and an ferryl oxygen on the heme iron was also encountered for the mutants (N70V and N70D) lacking the interactions to fix the distal His (Mukai et al., 1997). In these mutants, less basicity and improper orientation of the imidazole ring of the distal His disrupt the hydrogen bond to the ferryl oxygen. Thus, it is most likely that the less basicity and positional change of the distal residue found for the H42E mutant weaken or disrupt the hydrogen bond between the ferryl oxygen and $O_\epsilon H$ atom of the distal Glu residue, which led to the retardation of the reaction rate with a substrate.

Peroxygenase Activity. In sharp contrast to the decreases in peroxidase activity by the replacement of the distal His with Glu, the peroxygenase activities of the H42E mutant significantly increased (Table 2). The thioanisole sulfoxidation rate increased 50-fold for the H42E mutant and the activity of styrene epoxidation was enhanced by approximately 3 orders of magnitude. Such an enhancement in peroxygenase activity was also reported in the HRP mutants bearing a small-size amino acid residue at the distal cavity (Newmyer & Ortiz de Montellano, 1995). These mutations make the ferryl oxygen more accessible to thioanisole or styrene oxide and thereby facilitates ferryl oxygen transfer to the substrates (Newmyer & Ortiz de Montellano, 1995). In this study, the replacement of the His residue by Glu, which has smaller van der Waals volume (85.9 cm^3 mol^{-1}) than that of His (98.8 cm^3 mol^{-1}), enlarged the distal cavity in the H42E mutant. The enlarged distal cavity for the H42E mutant was also suggested by the lower enantioselectivities than that of wild-type enzyme (Table 2), which corresponds to the decreased steric restriction in the distal space. It should be noted here that the thioanisole sulfoxidation activities of the distal His mutants we prepared in this study were much higher than those of the mutants in which the distal His is replaced with Ala (H42A) or Val (H42V) residue. The H42A or H42V mutation increases the rate of thioanisole sulfoxidation only 10-fold (Newmyer & Ortiz de Montellano, 1995). Interestingly, F41A mutant bearing Ala residue at the position of Phe41 exhibited rather higher thioanisole sulfoxidation activity (Newmyer & Ortiz de Montellano, 1995). This mutant has the distal His and its compound I formation rate was almost the same as that for native enzyme. Comparison of the thioanisole sulfoxidation rates of the H42A and H42V mutations with that of the F41A mutant indicates that the rate effects of the replacement of the distal His with Ala or Val are not simply due to enlargement of the active site cavity (Newmyer & Ortiz de Montellano, 1995). Since the compound I formation in the H42A or H42V mutant was quite slow and this process becomes partly rate limiting in the thioanisole sulfoxidation reaction for the H42A or H42V mutant, their thioanisole sulfoxidation rates are moderately increased even though these mutants has the enlarged distal cavity (Newmyer & Ortiz de Montellano, 1995). On the other hand, the H42E and F41A mutants have a catalytic amino acid residue which facilitates the formation of compound I and, also, the enlarged distal cavity would drastically accelerate the thioanisole sulfoxidation. The contribution of the distal catalytic amino acid to thioanisole sulfoxidation reaction was confirmed by the observation that the H42Q mutant, like the H42A and H42V mutants, exhibited a severely depressed compound I formation rate and poor thioanisole sulfoxidation activity.

Although the activity enhancement was found for both of thioanisole sulfoxidation and styrene epoxidation, more drastic increase in the reaction rates are observed for styrene epoxidation and the H42Q mutant also exhibited enhanced epoxidation activity, compared to that of the native enzyme. As Newmyer and Ortiz de Montellano (1995) pointed out, styrene epoxidation reaction requires intimate contact of the ferryl oxygen with both carbons of the π-bond rather than simply with a sulfur electron pair and is therefore more sterically demanding than thioanisole sulfoxidation. However, the activity of the H42E mutant was much higher than that of H42Q, suggesting that a catalytic amino acid residue in the distal cavity is also requisite to promote the epoxidation reaction. In other words, the formation of compound I is a crucial step for styrene epoxidation as well as the accessibility of the substrate.

In summary, we have demonstrated that the distal Glu can play a role as a general acid-base catalyst in the peroxidase and peroxygenase reaction, in spite of the low basicity and improper orientation of the Glu residue. Another characteristic feature in the function of the mutants is the enhancement of the peroxygenase activity, due to the enlarged distal cavity caused by the amino acid substitution. These observations indicate that the distal amino acid residue is essential for function of peroxidases and subtle conformational changes around the distal cavity would control the catalytic reactions in peroxidase.

ACKNOWLEDGMENT

We are obliged to Prof. Yoshihito Watanabe (Institute for Molecular Science) for help of the peroxygenase activity experiments and his valuable discussion. We are thankful to Dr. Hiroshi Hori (Osaka University) for the EPR measurement. We are also grateful to Prof. Ryu Makino (Rikkyo University) for the redox potential measurement. We are obliged to Dr. Kiyohiro Imai (Osaka University) for assistance with the stopped-flow experiment. M.T. was supported by Research Fellowships of Japan Society for the Promotion of Science for Young Scientists.

REFERENCES

Al-Mustafa, J., & Kincaid, J. R. (1994) *Biochemistry 33*, 2191−2197.

Clarke, J., & Shannon, L. M. (1976) *Biochim. Biophys. Acta 427*, 428−442.

Cormier, M. J., & Prichard, P. M. (1968) *J. Biol. Chem. 243*, 4706−4714.

Dawson, J. H., & Sono, M. (1987) *Chem. Rev. 87*, 1255−1276.

Dunfold, H. B. (1991) in *Peroxidases in Chemistry and Biology*, (Everse, J. E., Everse, K. E., & Grisham, M. B., Eds.) Vol. II, pp 1−24, CRC Press, Boca Raton.

Edwards, S. L., Raag, R., Wariishi, H., Gold, M. H., & Poulos, T. L. (1993) *Proc. Natl. Acad. Sci. U.S.A. 90*, 750−754.

Erman, J. E., Vitello, L. B., Miller, M. A., & Kraut, J. (1992) *J. Am. Chem. Soc. 114*, 6592−6593.

Erman, J. E., Vitello, L. B., Miller, M. A., Shaw, A., Brown, K. A., & Kraut, J. (1993) *Biochemistry 32*, 9798−9806.

Farhangrazi, Z. S., Copeland, B. R., Nakayama, T., Amachi, T., Yamazaki, I., & Powers, L. S. (1994) *Biochemistry 33*, 5647−5652.

Finzel, B. C., Poulos, T. L., & Kraut, J. (1984) *J. Biol. Chem. 259*, 13027−13036.

Fruetel, J. A., Collins, J. R., Camper, D. L., Loew, G. H., & Ortiz de Montellano, P. R. (1992) *J. Am. Chem. Soc. 114*, 6987−6993.

Fruetel, J. A., Chang, Y.-Y., Collins, J. R., Loew, G. H., & Ortiz de Montellano, P. R. (1994) *J. Am. Chem. Soc. 116*, 11643−11648.

Fukuyama, K., Kunishima, N., Amada, F., Kubota, T., & Matsubara, H. (1995) *J. Biol. Chem. 270*, 21884−21892.

Gazaryan, I. G., Doseeva, V. V., Galkin, A. G., & Tishkov, V. I. (1994) *FEBS Lett. 354*, 248−250.

Greenfield, N., & Fasman, G. D. (1969) *Biochemistry 8*, 4108−4116.

Haschke, R. H., & Friedhoff, J. M. (1978) *Biochem. Biophys. Res. Commun. 80*, 1039−1042.

Hasinoff, B. B., & Dunfold, H. B. (1970) *Biochemistry 9*, 4930−4939.

Job, D., & Dunfold, H. B. (1976) *Eur. J. Biochem. 66*, 607−614.

Kunishima, N., Fukuyama, K., Matsubara, H., Hatanaka, H., Shibano, Y., & Amachi, T. (1994) *J. Mol. Biol. 235*, 331−344.

MacLeod, A. M., Lindhorst, T., Withers, S. G., & Warren, R. A. J. (1994) *Biochemistry 33*, 6371−6376.
Makino, R., Iizuka, T., Sakaguchi, K., & Ishimura, Y. (1982) in *Oxygenase and Oxygen Metabolism* (Nozaki, M., Yamamoto, S., Oshimura, Y., Coon, M. J., Ernster, L., & Estabrook, R. W., Eds.) pp 467−477, Academic Press, New York.
Makino, R., Uno, T., Nishimura, Y., Iizuka, T., Tsuboi, M., & Ishimura, Y. (1986) *J. Biol. Chem. 261*, 8376−8382.
Morishima, I., Kurono, M., & Shiro, Y. (1986) *J. Biol. Chem. 261*, 9391−9399.
Mukai, M., Nagano, S., Tanaka, M., Ishimori, K., Morishima, I., Ogura, T., Watanabe, Y., & Kitagawa, T. (1997) *J. Am. Chem. Soc. 119*, 1758−1766.
Nagano, S., Tanaka, M., Watanabe, Y., & Morishima, I. (1995) *Biochem. Biophys. Res. Commun. 207*, 417−423.
Nagano, S., Tanaka, M., Ishimori, K., Watanabe, Y., & Morishima, I. (1996) *Biochemistry 35*, 14251−14258.
Newmyer, S. L., & Montellano, P. R. O. (1995) *J. Biol. Chem. 270*, 19430−19438.
Newmyer, S. L., & Montellano, P. R. O. (1996) *J. Biol. Chem. 271* 14891−14896.
Ogawa, S., Shiro, Y., & Morishima, I. (1979) *Biochem. Biophys. Res. Commun. 90*, 674−678.
Ozaki, S., & Montellano, P. R. O. (1994) *J. Am. Chem. Soc. 116*, 4487−4488.
Ozaki, S., & Montellano, P. R. O. (1995) *J. Am. Chem. Soc. 117*, 7056−7064.
Patterson, W. R., & Poulos, T. L. (1995) *Biochemistry 34*, 4331−4341.
Paul, K. G., Theorell, H., & Akesson, A. (1953) *Acta Chem. Scand. 7*, 1284−1287.
Petersen, J. F. W., Kadziola, A., & Larsen, S. (1994) *FEBS Lett. 339*, 291−296.
Poulos, T. L., & Kraut, J. (1980) *J. Biol. Chem. 255*, 8199−8205.
Poulos, T. L., Edwards, S. L., Wariishi, H., & Gold, M. G. (1993) *J. Biol. Chem. 268*, 4429−4440.
Rodriguez-Lopez, J. N., Smith, A. T., & Thorneley, R. N. F. (1996) *J. Bioinorg. Chem. 1*, 136−142.
Sawaki, Y., & Foote, C. S. (1979) *J. Am. Chem. Soc. 101*, 6292−6296.
Schuller, D. J., Ban, N., van Huystee, R. B., McPherson, A., & Poulos, T. L. (1996) *Structure 4*, 311−321.
Schulz, C. E., Devaney, P. W., Winkler, H., Debrunner, P. G., Doan, N., Chiang, R., Rutter, R., & Hager, L. P. (1979) *FEBS Lett. 103*, 102−105.
Sitter, A. J., Reczek, C. M., & Terner, J. (1985) *J. Biol. Chem. 260*, 7515−7520.
Smith, A. T., Sanders, S. A., Thorneley, R. N. F., Burke, J. F., & Bray, R. R. C. (1992) *Eur. J. Biochem. 207*, 507−519.
Smulevich, G., Paoli, M., Burke, J. F., Sanders, S. A., Thorneley, R. N. F., & Smith, A. T. (1994) *Biochemistry 33*, 7398−7407.
Sun, W., Kadima, T. A., Pickard, M. A., & Dunfold, H. B. (1994) *Biochem. Cell Biol. 72*, 321−331.
Sundaramoorthy, M., Kishi, K., Gold, M. H., & Poulos, T. L. (1994) *J. Biol. Chem. 269*, 32759−32767.
Sundaramoorthy, M., Terner, J., & Poulos, T. L. (1995) *Structure 3*, 1367−1377.
Tanaka, M., Ishimori, K., & Morishima, I. (1996) *Biochem. Biophys. Res. Commun. 227*, 393−399.
Tanaka, M., Nagano, S., Ishimori, K., & Morishima, I. (1997) *Biochemistry* (in press).
Teraoka, J., & Kitahawa, T (1981) *J. Biol. Chem. 256*, 3969−3977.
Vitello, L. B., Erman, J. E., Miller, M. A., Mauro, J. M., & Kraut, J. (1992) *Biochemistry 31*, 11524−11535.
Welinder, K. G. (1979) *Eur. J. Biochem. 96*, 483−502.
Yamada, H., Makino, R., & Yamazaki, I. (1975) *Arch. Biochem. Biophys. 169*, 344−353.
Yamazaki, I., & Yokota, K. (1973) *Mol. Cell. Biochem. 2*, 39−52.

BI970906Q